© 2021. Published by The Company of Biologists Ltd | Development (2021) 148, dev198838. doi:10.1242/dev.198838

STEM CELLS AND REGENERATION

RESEARCH ARTICLE

Arid1a regulates cell cycle exit of transit-amplifying cells by inhibiting the Aurka-Cdk1 axis in mouse incisor

Jiahui Du[1,2], Junjun Jing[1], Shuo Chen[1], Yuan Yuan[1], Jifan Feng[1], Thach-Vu Ho[1], Prerna Sehgal[1], Jian Xu[1], Xinquan Jiang[2] and Yang Chai[1,*]

ABSTRACT

Stem cells self-renew or give rise to transit-amplifying cells (TACs) that differentiate into specific functional cell types. The fate determination of stem cells to TACs and their transition to fully differentiated progeny is precisely regulated to maintain tissue homeostasis. Arid1a, a core component of the switch/sucrose nonfermentable complex, performs epigenetic regulation of stage- and tissue-specific genes that is indispensable for stem cell homeostasis and differentiation. However, the functional mechanism of Arid1a in the fate commitment of mesenchymal stem cells (MSCs) and their progeny is not clear. Using the continuously growing adult mouse incisor model, we show that Arid1a maintains tissue homeostasis through limiting proliferation, promoting cell cycle exit and differentiation of TACs by inhibiting the Aurka-Cdk1 axis. Loss of *Arid1a* overactivates the Aurka-Cdk1 axis, leading to expansion of the mitotic TAC population but compromising their differentiation ability. Furthermore, the defective homeostasis after loss of *Arid1a* ultimately leads to reduction of the MSC population. These findings reveal the functional significance of Arid1a in regulating the fate of TACs and their interaction with MSCs to maintain tissue homeostasis.

KEY WORDS: Arid1a, Mesenchymal stem cells, Transit-amplifying cells, Cell cycle, Mitosis

INTRODUCTION

Stem cells reside in a variety of adult tissues, such as the mammalian hematopoietic and nervous systems, intestine and hair follicle (Morrison et al., 1997). During tissue homeostasis and regeneration, stem cells can self-renew or exit their niche environment to differentiate into specific cell types, contributing to diverse tissue functions (Morrison and Spradling, 2008). The biology of stem cells has been the subject of intense focus as they play a crucial role in tissue development, with potential applications for the treatment of numerous diseases. For example, bone marrow and peripheral blood stem cell transplants have been used for restoring stem cells in patients after chemotherapy and/or radiation therapy for over 40 years (Childs et al., 2000; Thomas, 1975). In many tissues, between stem cells and terminally differentiated cells there is an undifferentiated population of cells that undergo mitosis at a rapid rate, termed transit-amplifying cells (TACs) (Hsu et al., 2014). Once stem cells exit their quiescent state, they initiate proliferation and immediately become TACs. Recently, the importance of TACs in stem cell homeostasis has been gradually unveiled (Zhang and Hsu, 2017). For example, TACs can serve as a signaling center and integrator of stem cell niche components, orchestrating tissue growth in the hair follicle (Hsu et al., 2014), and TACs in the hematopoietic system renew themselves and sustain long-term, steady-state hematopoiesis (Busch et al., 2015; Sun et al., 2014). Therefore, the cell fate commitment of TACs is an important event in the function of stem cells in tissue homeostasis.

The fate determination and transition of stem cells to TACs, as well as to their fully differentiated progeny, are precisely regulated by intrinsic and extrinsic factors with dynamic transcription activity of stage-specific genes (Morrison et al., 1997). Proliferation-associated genes need to be suppressed, whereas particular lineage-specific transcription regulators need to be activated during differentiation (Ruijtenberg and van den Heuvel, 2016). Multiple conserved signaling pathways have emerged as crucial regulators of these events. For example, Notch-Wnt-Shh-Smad signaling circuits control self-renewal and differentiation of hematopoietic stem cells (Blank et al., 2008), and stromal cells secrete WNT, Notch and BMP signaling factors as they maintain epithelial stem cells (Chacon-Martinez et al., 2018). In addition, growing evidence has shown that epigenetic modifications, including DNA methylation, histone modification, RNA-mediated regulation and chromatin remodeling, are indispensable for transcriptional regulation during the fate determination of stem/progenitor cells (Cakouros and Gronthos, 2020; Wu and Sun, 2006). The switch/sucrose nonfermentable (SWI/SNF) chromatin remodeling complex is one important family of ATP-dependent chromatin remodelers. This complex is comprised of multiple protein subunits and it conducts the translocation of nucleosomes and regulates gene transcription directly (Wilson and Roberts, 2011). Arid1a, a core component of the SWI/SNF complex, can directly bind to gene promoters and enhancers through its DNA-binding domain to regulate stage- and tissue-specific gene expression (Hota and Bruneau, 2016). Previous studies have shown that Arid1a is indispensable for the homeostasis and differentiation of hematopoietic and intestinal stem cells (Han et al., 2019; Hiramatsu et al., 2019). However, the function of Arid1a in the fate commitment of mesenchymal stem cells (MSCs) and their progeny is not clear. A previous study has shown that loss of *Arid1a* in cranial neural crest (CNC) cells leads to craniofacial bone defects, suggesting that Arid1a may also play a crucial role in the fate commitment of MSCs and their progeny (Chandler and Magnuson, 2016).

The mouse incisor is a continuously growing organ, and the stem cells at its proximal end fuel its lifelong growth (Seidel et al., 2010; Zhao et al., 2014). Genetic lineage tracing has identified Gli1+ cells residing in the proximal end of the incisor surrounding the neurovascular bundle as typical MSCs (Zhao et al., 2014). They can give rise to mesenchymal TACs, which then differentiate into odontoblasts and dental pulp cells in a specific proximal-to-distal

[1]Center for Craniofacial Molecular Biology, University of Southern California, Los Angeles, CA, 90033, USA. [2]Department of Prosthodontics, Shanghai Ninth People's Hospital, College of Stomatology, Shanghai Jiao Tong University School of Medicine, Shanghai, 200011, China.

*Author for correspondence (ychai@usc.edu)

Y.C., 0000-0003-2477-7247

Handling Editor: Liz Robertson
Received 18 November 2020; Accepted 18 March 2021

Development (2021) 148, dev198838. doi:10.1242/dev.198838

order (Feng et al., 2011; Kaukua et al., 2014; Menon et al., 2019; Zhao et al., 2014). In addition, a recent study has shown that mesenchymal TAC properties and TAC-to-MSC feedback can be regulated by another chromatin modifier, polycomb repressive complex 1 (PRC1), in adult mouse incisor (An et al., 2018). Therefore, the rapid renewal rate combined with the directional transition from MSCs to TACs and then to odontoblasts make the mouse incisor an optimal model for studying the role of Arid1a in the fate commitment and homeostasis of MSCs and their progeny.

In this study, we show that Arid1a expression co-localizes with TACs and is mutually exclusive with MSCs in the adult mouse incisor. Using *Gli1-CreER;Arid1a*$^{fl/fl}$ mice, we discovered that loss of *Arid1a* impairs the growth and homeostasis of the mouse incisor. Furthermore, Arid1a maintains tissue homeostasis through promoting cell cycle exit and differentiation of TACs. We have also identified that Arid1a binds to the promoters of *Aurka*, *Ccnb1* and *Cdk1* and might participate in their transcriptional repression during the mitotic exit of TACs. Loss of *Arid1a* overactivates the Aurka-Cdk1 axis, leading to expansion of the mitotic TAC population but compromising its differentiation ability. Furthermore, the defective homeostasis after loss of *Arid1a* ultimately leads to reduction of the MSC population. Our findings expand our knowledge of the epigenetic regulation of Arid1a in maintaining tissue homeostasis through mediating TAC fate determination and TAC-MSC interaction.

RESULTS

Arid1a is expressed by cell populations adjacent to, but mutually exclusive with, MSCs in the adult mouse incisor

To investigate the role of Arid1a during the fate commitment of MSCs and their contribution to tissue homeostasis in the adult mouse incisor, we first evaluated the expression pattern of Arid1a in the proximal region of the incisor. Interestingly, we found that Arid1a is expressed in TACs, preodontoblasts, odontoblasts and dental pulp cells in the adult mouse incisor but not near the neurovascular bundle, in which MSCs reside (Fig. 1A,B). Arid1a is also present in dental epithelial cells in the adult mouse incisor (Fig. 1B). To elucidate the relationship between Arid1a+ cells and Gli1+ MSCs in the adult mouse incisor, we analyzed co-localization of Arid1a and Gli1 in 1-month-old *Gli1-lacZ* mice. The Arid1a+ and Gli1+ populations were mutually exclusive (Fig. 1C,D). It is known that Gli1+ MSCs exit from their niche and replenish adjacent TACs to maintain tissue homeostasis (Zhao et al., 2014). To determine the relationship between TACs and Arid1a+ cells, we performed double staining of Arid1a and Ki67, a marker labeling cycling cells, and found that most TACs express Arid1a in the proximal region of the mouse incisor in 1-month-old mice (Fig. 1E,F). The strategic location of Arid1a+ cells suggests that Arid1a might play a specific role in regulating the function of TACs as well as the TAC-MSC interaction in regulating tissue homeostasis.

Deletion of *Arid1a* impairs incisor growth and tissue homeostasis

To test our hypothesis that Arid1a serves a crucial function in the homeostasis of TACs and MSCs in the adult mouse incisor, we generated *Gli1-CreER;Arid1a*$^{fl/fl}$ mice. We induced Cre activity with tamoxifen at 1 month of age, and found that Arid1a was efficiently deleted in the incisor mesenchyme 2 weeks after induction (Fig. S1A-D). To investigate the dynamic change in the growth rate of the incisor after loss of *Arid1a*, we performed notch movement analysis in control and *Gli1-CreER;Arid1a*$^{fl/fl}$ mice. A notch was made in the incisor enamel above the gingival margin 2 weeks after tamoxifen induction. We found that the notch movement was significantly slower in *Gli1-CreER;Arid1a*$^{fl/fl}$ mice compared with control mice at 10 days, suggesting that loss of *Arid1a* impaired the growth rate of the mouse incisor (Fig. 2A-G).

Histologically, at 1 month after induction, we observed that polarization of odontoblasts (Fig. 2H,I) and expression of odontoblast differentiation marker *Dspp* (Fig. 2J,K) initiated more proximally in *Gli1-CreER;Arid1a*$^{fl/fl}$ mice compared with control samples. This defect was increasingly severe with formation of stacked dentin in the proximal region of the incisor at 2 months after induction (white asterisk, Fig. 2L,M). Furthermore, we found that the proximal odontoblasts in *Gli1-CreER;Arid1a*$^{fl/fl}$ mice were not as dense as those in control samples and lost the normally tight cell-cell contact (green arrow, Fig. 2M). Later, at 3 months post-induction, severe disorganized dentin was found in the dental pulp cavity of *Gli1-CreER;Arid1a*$^{fl/fl}$ mouse incisors (black arrow, Fig. S2). In detail, we found the disorganized dentin together with enamel in the proximal region (white asterisk, Fig. 2N,O) with disordered alignment of odontoblasts and cervical loop (green dashed line, Fig. 2O) in *Gli1-CreER;Arid1a*$^{fl/fl}$ mouse incisor. Considering the inhibited growth rate after loss of *Arid1a* in notch movement experiments, we speculated that loss of *Arid1a* may lead to defective proximal-distal migration of odontoblasts and an insufficiency of new odontoblasts, resulting in disrupted tissue homeostasis.

As Gli1+ cells contribute to both mesenchymal and epithelial lineages in the incisor (Zhao et al., 2014), Arid1a was lost in both of these tissues in *Gli1-CreER;Arid1a*$^{fl/fl}$ mice. Previous studies have

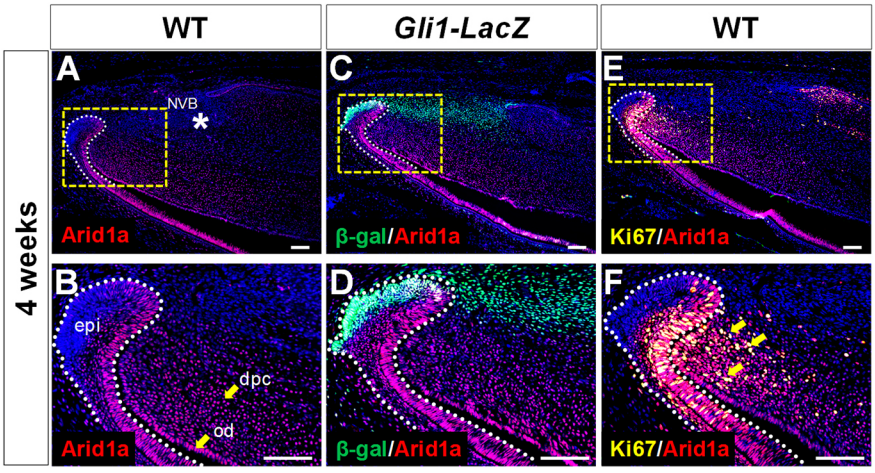

Fig. 1. Arid1a is expressed by cell populations adjacent to, but mutually exclusive from, MSCs in the adult mouse incisor. (A,B) Arid1a immunofluorescence (red) in a 1-month-old wild-type (WT) mouse. Box in A is shown at higher magnification in B. *n*=3. (C,D) Co-immunofluorescence of Arid1a (red) and Gli1 (stained by β-gal in green) of incisor from 1-month-old *Gli1-lacZ* mouse. Box in C is shown at higher magnification in D. *n*=3. (E,F) Co-immunofluorescence of Arid1a (red) and Ki67 (yellow) of incisor from 1-month-old WT mouse. Box in E is shown at higher magnification in F. *n*=3. Yellow arrows indicate positive signal. Asterisk indicates no signal. White dotted line outlines the cervical loop. dpc, dental pulp cell; epi, epithelium; NVB, neurovascular bundle; od, odontoblast. Scale bars: 100 µm.

Development (2021) 148, dev198838. doi:10.1242/dev.198838

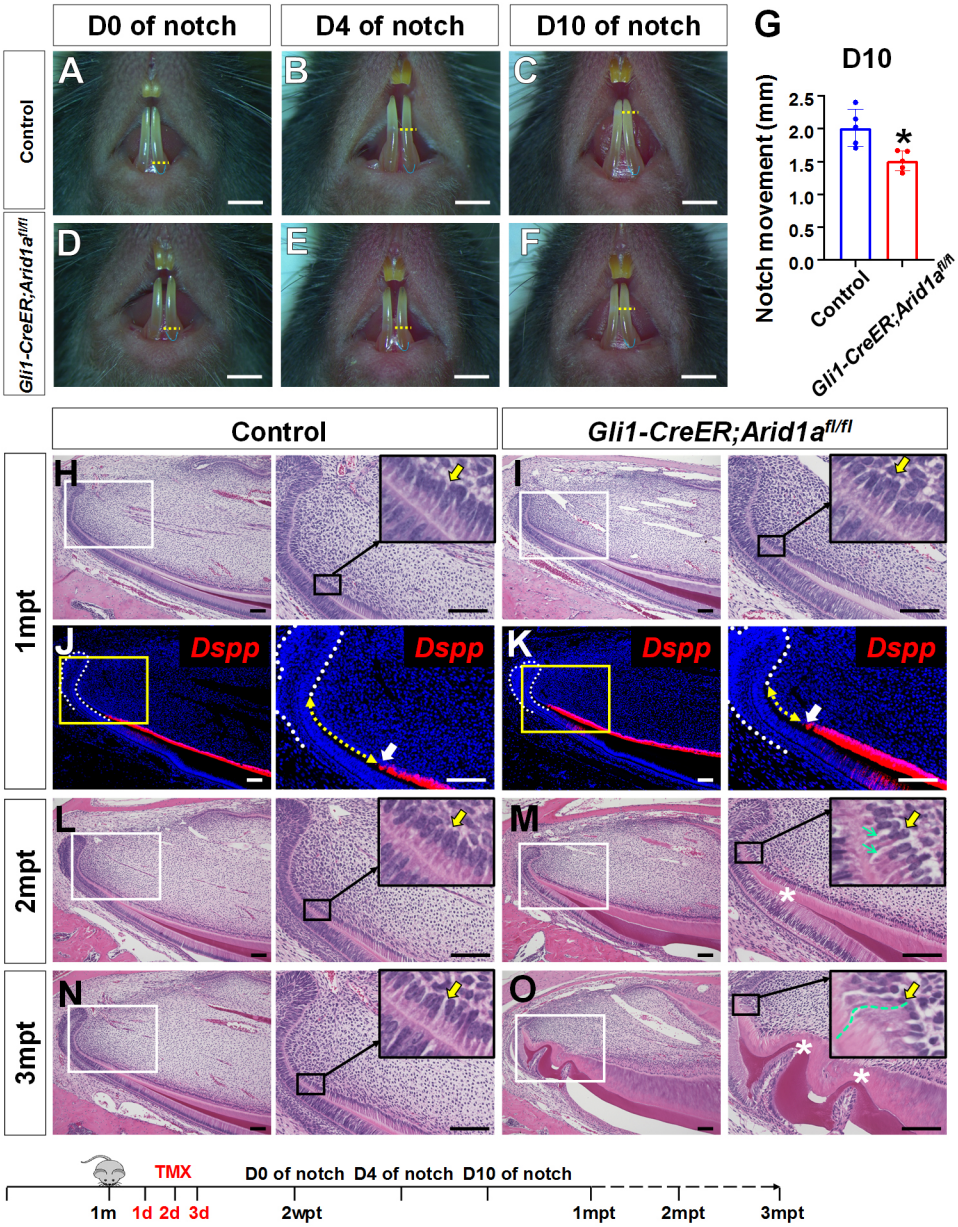

Fig. 2. Loss of *Arid1a* in the Gli1+ lineage results in impaired incisor growth and homeostasis. (A-F) Notch movement in control (A-C) and *Gli1-CreER;Arid1a*$^{fl/fl}$ (D-F) mice 2 weeks after induction. All the notches were made in the right side of the incisor above the gingival margin; the yellow dotted line on the left shows the level of the notch movement. Blue line shows the outline of the gingival margin. *n*=5. (G) Quantification of the notch movement in control and *Gli1-CreER;Arid1a*$^{fl/fl}$ mice at D10. Data are mean ±s.d., *n*=5, unpaired two-tailed Student's *t*-test, **P*<0.05. (H-O) H&E staining of incisors from control and *Gli1-CreER;Arid1a*$^{fl/fl}$ mice at 1 month (H,I), 2 months (L,M) and 3 months (N,O) after induction. Yellow arrows indicate the initiation of odontoblast polarization. Green arrows in M indicate the increased space in the odontoblasts. Green curved dashed line in O indicates the disordered alignment of odontoblasts. White asterisks in M and O indicate stacked and distorted dentin. *n*=3. *In situ* hybridization of *Dspp* (red; J,K) on incisors of control and *Gli1-CreER;Arid1a*$^{fl/fl}$ mice 1 month after induction. White dotted line outlines cervical loop. White arrows indicate the initiation of odontoblast differentiation. Yellow dotted two-way arrow shows the distance between the bending point of the cervical loop and the initiation of odontoblast differentiation. *n*=3. Boxes in H-O are shown at higher magnification on the right. Schematic at the bottom indicates induction and notch creation protocol. mpt, month post-tamoxifen injection; wpt, week post-tamoxifen injection. Scale bars: 2 mm (A-F); 100 µm (H-O).

shown that Sox2+ cells are epithelial stem cells in the adult mouse incisor that can contribute to all epithelial cell lineages (Arnold et al., 2011; Juuri et al., 2013, 2012). To rule out loss of *Arid1a* in the dental epithelium as the cause of the mesenchymal defects in *Gli1-CreER;Arid1a*$^{fl/fl}$ mice, we generated *Sox2-CreER;Arid1a*$^{fl/fl}$ mice. We induced the Cre activity with tamoxifen from 1 month of age. However, we did not observe any apparent defects of odontoblast polarization or differentiation in *Sox2-CreER;Arid1a*$^{fl/fl}$ mice compared with control samples 1 month after induction (Fig. S3). These data confirm that Arid1a in the dental mesenchyme, but not the dental epithelium, is indispensable for maintaining tissue homeostasis of the adult mouse incisor.

Loss of *Arid1a* leads to expanded TACs with compromised odontoblast differentiation and reduction of the MSC population

Incisor growth and dentin formation are fueled by the proliferation and differentiation of MSCs in the proximal region of the tooth (Zhao et al., 2014). To investigate the cellular mechanism underlying the incisor growth and homeostasis defects following the loss of *Arid1a*, we examined the proliferation and differentiation activity of Gli1+ MSCs. Surprisingly, although the growth rate was reduced in the mouse incisor as early as 2 weeks after induction (Fig. 2A-G), the number of mesenchymal TACs increased significantly in *Gli1-CreER;Arid1a*$^{fl/fl}$ mice compared with control mice at the same time point (Fig. 3A-E). Then, using tdTomato (tdT) as a reporter, we evaluated the differentiation of Gli1+ MSCs and found that the length of tdT+ dental pulp cell contribution significantly decreased in *Gli1-CreER;Arid1a*$^{fl/fl}$*;tdT* mice compared with control samples 2 weeks after induction (Fig. 3F-H). Therefore, we hypothesized that the transition from TAC proliferation to differentiation may be defective following the loss of *Arid1a*.

To further test our hypothesis, we utilized EdU tracing to assess the ability of TACs to differentiate into odontoblasts after loss of *Arid1a*. We labeled TACs in the DNA synthesis phase with EdU 48 h before euthanizing the mice, such that the overlapping length of Dspp+ odontoblasts and EdU+ labeled cells represented the odontoblast differentiation rate of TACs during this period. We

Development (2021) 148, dev198838. doi:10.1242/dev.198838

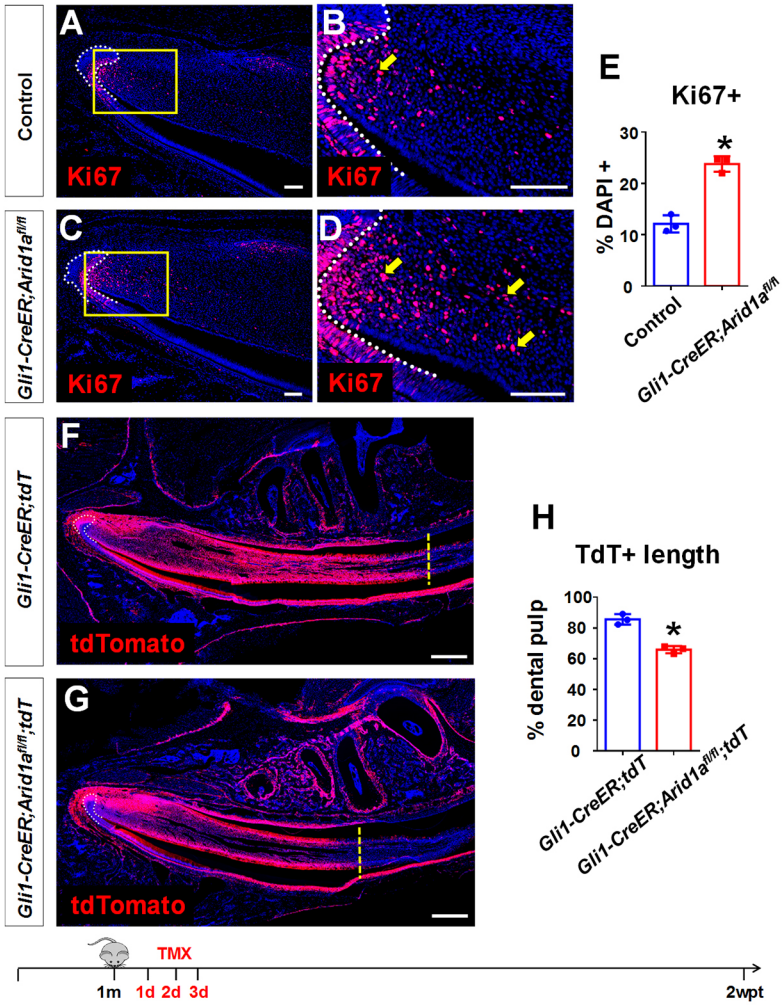

Fig. 3. Loss of *Arid1a* leads to expanded TAC region but compromised differentiation ability. (A-D) Ki67 immunostaining of incisors from control (A,B) and *Gli1-CreER;Arid1a*$^{fl/fl}$ mice (C,D) 2 weeks after induction. B and D represent high-magnification images of boxes in A and C, respectively. White dotted line outlines cervical loop. Yellow arrows indicate positive signal. *n*=3. (E) Quantification of the percentage of Ki67+ cells in dental mesenchyme of incisors from control and *Gli1-CreER;Arid1a*$^{fl/fl}$ mice 2 weeks after induction. Data are mean±s.d., *n*=3, unpaired two-tailed Student's *t*-test, **P*<0.05. (F,G) Differentiation rate of Gli1+ MSCs in *Gli1-CreER;tdTomato* and *Gli1-CreER;Arid1a*$^{fl/fl}$*;tdTomato* mice 2 weeks after induction. *n*=3. White dotted line outlines the cervical loop. Yellow dashed line represents the front of differentiation. (H) Quantification of tdTomato signal in *Gli1-CreER;tdTomato* and *Gli1-CreER;Arid1a*$^{fl/fl}$*;tdTomato* mice 2 weeks after induction. Data are mean±s.d., *n*=3, unpaired two-tailed Student's *t*-test, **P*<0.05. Schematic at the bottom indicates induction protocol. wpt, week post-tamoxifen injection. Scale bars: 100 µm (A-D); 500 µm (F-G).

observed that the differentiation of TACs was inhibited significantly in *Gli1-CreER;Arid1a*$^{fl/fl}$ mice compared with control samples 2 weeks after induction (Fig. 4A-E). Given that loss of *Arid1a* leads to no apparent change in apoptosis (Fig. S4A-E), we hypothesized that loss of *Arid1a* leads to impaired ability of labeled TACs to exit the cell cycle. We visualized EdU-labeled cells with Ki67, a marker labeling cycling cells, to compare the cell cycle exit rate of TACs after loss of *Arid1a* during this period. As expected, more TACs remained arrested in the cell cycle during the 48 h period under study in *Gli1-CreER;Arid1a*$^{fl/fl}$ mice compared with control samples (Fig. 4F-J).

Interestingly, we also noticed that the loss of *Arid1a* leads to reduction of the Gli1+ MSC population 2 weeks after induction, suggesting that although Arid1a is not expressed in Gli1+ MSC population, loss of *Arid1a* in TACs and other dental pulp cells may trigger feedback that ultimately leads to reduction of the Gli1+ MSC population in the incisors of *Gli1-CreER;Arid1a*$^{fl/fl}$ mice (Fig. S5A-E). Taken together, our results suggest that loss of *Arid1a* impairs cell cycle exit of TACs, which leads to an expanded TAC population alongside compromised odontoblast differentiation and may ultimately cause reduction of the MSC population.

Arid1a inhibits the Aurka-Cdk1 axis during TAC cell cycle exit

To further investigate how Arid1a regulates cell cycle exit and differentiation of TACs, we conducted RNA-sequencing analysis to compare the transcriptional profiles in the proximal region of the incisor mesenchyme in control and *Gli1-CreER;Arid1a*$^{fl/fl}$ mice 2 weeks after induction. PCA analysis of the RNA-sequencing data showed well-separated transcriptional profiles of the control and *Gli1-CreER;Arid1a*$^{fl/fl}$ incisors (Fig. S6A) with a total of 370 downregulated and 435 upregulated genes ($P \leq 0.01$; fold change <-1.5 or >1.5) in *Arid1a* mutants compared with controls (Fig. S6B). As expected, the cell cycle pathway was among the most changed pathways (Fig. S6C). We also noticed that a set of mitotic-associated genes was upregulated consistently after loss of *Arid1a* (Fig. S6D). The dynamic regulation of Aurka-Ccnb1-Cdk1 axis plays a central role during mitosis (Cazales et al., 2005). We found that the gene expression levels of *Aurka*, *Ccnb1* and *Cdk1* were upregulated significantly in the TAC region after loss of *Arid1a* 2 weeks after induction using RNAscope *in situ* hybridization and quantitative reverse transcription PCR (qPCR) analyses (Fig. 5A-L, Q). To test whether the cell cycle exit defects of TACs were caused by overactivation of the Aurka-Ccnb1-Cdk1 axis, we assessed the mitotic TACs after loss of *Arid1a* using mitosis phase marker pHH3. We found that the number of mitotic TACs increased significantly after loss of *Arid1a*, accounting for the majority of the increase in Ki67+ cells in the *Gli1-CreER;Arid1a*$^{fl/fl}$ mouse incisor (Fig. 5M-P, R). Also, we evaluated the mitotic exit of TACs during a 48 h period in control and *Gli1-CreER;Arid1a*$^{fl/fl}$ mice 2 weeks after induction and found that more EdU-labeled cells were undergoing mitosis in *Gli1-CreER;Arid1a*$^{fl/fl}$ mouse incisors than in control samples (Fig. 6A-E). Furthermore, the increase in the number of

Development (2021) 148, dev198838. doi:10.1242/dev.198838

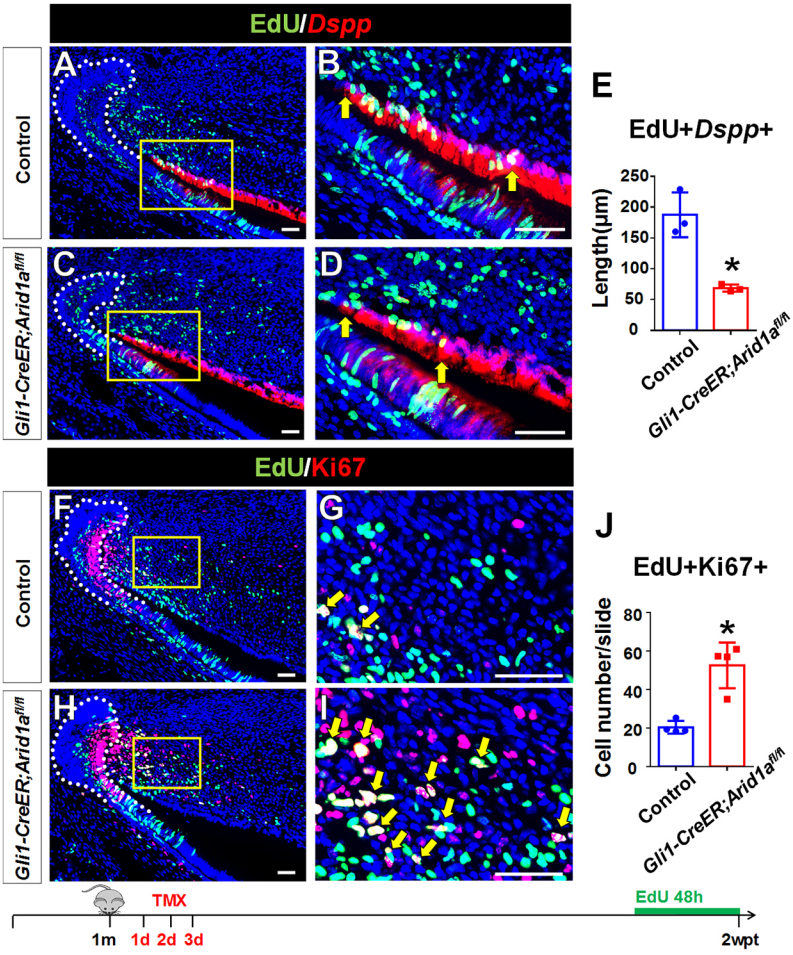

Fig. 4. Loss of *Arid1a* leads to defective TAC cell cycle exit. (A-D) RNAscope of *Dspp* (Red) and EdU staining (green) of incisors from control (A-B) and *Gli1-CreER;Arid1a*$^{fl/fl}$ mice (C-D) 2 weeks after induction. B, D represent high-magnification images of boxes in A, C, respectively. White dotted line outlines the cervical loop. *n*=3. (E) Quantification of the overlapping length of EdU-labeled *Dspp*+ cells (distance between yellow arrows) from control and *Gli1-CreER;Arid1a*$^{fl/fl}$ mouse incisors 2 weeks after induction. Data are mean±s.d., *n*=3, unpaired two-tailed Student's *t*-test, **P*<0.05. (F-I) Immunostaining of Ki67 (Red) and EdU staining (green) of incisors from control (F-G) and *Gli1-CreER;Arid1a*$^{fl/fl}$ mice (H-I) 2 weeks after induction. G, I represent high-magnification images of boxes in F, H, respectively. Yellow arrows indicate EdU+Ki67+ cells. White dotted line outlines the cervical loop. *n*=4. (J) Quantification of EdU+Ki67+ cells from control and *Gli1-CreER;Arid1a*$^{fl/fl}$ mouse incisors 2 weeks after induction. Data are mean±s.d., *n*=4, unpaired two-tailed Student's *t*-test, **P*<0.05. Schematic at the bottom indicates induction and EdU incorporation protocol. wpt, week post-tamoxifen injection. Scale bars: 50 µm.

EdU+PHH3+ cells was comparable with that of EdU+Ki67+ cells in *Gli1-CreER;Arid1a*$^{fl/fl}$ mouse incisors compared with control samples (Fig. 4J), suggesting the cell cycle exit defect may primarily affect cells undergoing mitosis. To exclude the possibility that more TACs are labeled by EdU at the start, leading to more cells undergoing mitosis or remaining in the cell cycle after 48 h, we evaluated the number of EdU+ cells 2 h after labeling. We found that, although the number of mitotic cells and the overall number of cycling cells in the TAC region were increased significantly at the same time point (Figs 5M-P and 3A-E), the number of cells in the DNA synthesis phase had not changed significantly (Fig. S7). This result suggested that TACs are most likely arrested in mitosis after loss of *Arid1a*, leading consequently to cell cycle exit and odontoblast differentiation defects.

To rule out the possibility that the TACs are trapped in an undifferentiated state due to an inability to respond to differentiation signals or failure to activate differentiation programs, we also investigated the effect of Arid1a deletion on the expression and function of major odontoblast lineage specifiers. Previous studies have shown that BMP (Shi et al., 2019) and WNT signaling (An et al., 2018; Jing et al., 2021) are indispensable for the odontoblast differentiation of TACs in the adult mouse incisor. We did not find any apparent effect on them, as indicated for BMP signaling by the expression levels of p-Smad1/5/9 (Fig. S8A-D) and for WNT signaling by Ccnd1 and *Axin2* (Fig. S8E-L). We also evaluated the expression level of Klf4, a crucial transcription factor for odontoblast differentiation in the mouse molar (Feng et al., 2017), and did not find any apparent effect on its expression level in the pre-odontoblast and odontoblast region after loss of *Arid1a* (Fig. S8M-P). These results suggested that the mitotic arrest of TACs is most likely cell-autonomous and the odontoblast differentiation defect is secondary.

Protein phosphatase 2A (PP2A) is one of the most crucial phosphatases involved in cell division. It can dephosphorylate CDK1 substrates and promote mitotic exit (Wlodarchak and Xing, 2016). When we used the PP2A activator SMAP to counteract the overactivation of the Aurka-Ccnb1-Cdk1 axis, the number of PHH3+ cells after loss of *Arid1a* was significantly reduced (Fig. 6F-L) and the defective differentiation of TACs into odontoblasts seen after loss of *Arid1a* was partially rescued (Fig. 6M-S).

Arid1a negatively regulates promoter activities of *Aurka*, *Ccnb1* and *Cdk1*

Previous studies have shown that Arid1a functionally binds to promoters and negatively or positively regulates the accessibility of transcription complexes such as RNA polymerase II and transcriptional repressors or activators (Liu et al., 2020; Suryo Rahmanto et al., 2016; Wilson et al., 2019). In order to test how Arid1a regulates the Aurka-Ccnb1-Cdk1 axis during cell cycle exit, we investigated Arid1a transcriptional regulation of *Aurka*, *Ccnb1 and Cdk1* at the proximal promoter regions using dual luciferase reporter assays. We found that knocking down Arid1a using siRNA in the ST2 mesenchymal stromal cell line led to significant upregulation of *Aurka*, *Ccnb1* and *Cdk1* promoter activities (Fig. 7A), suggesting that Arid1a represses their transcriptional activity. We further determined whether Arid1a directly binds to the promoter regions of *Aurka*,

Development (2021) 148, dev198838. doi:10.1242/dev.198838

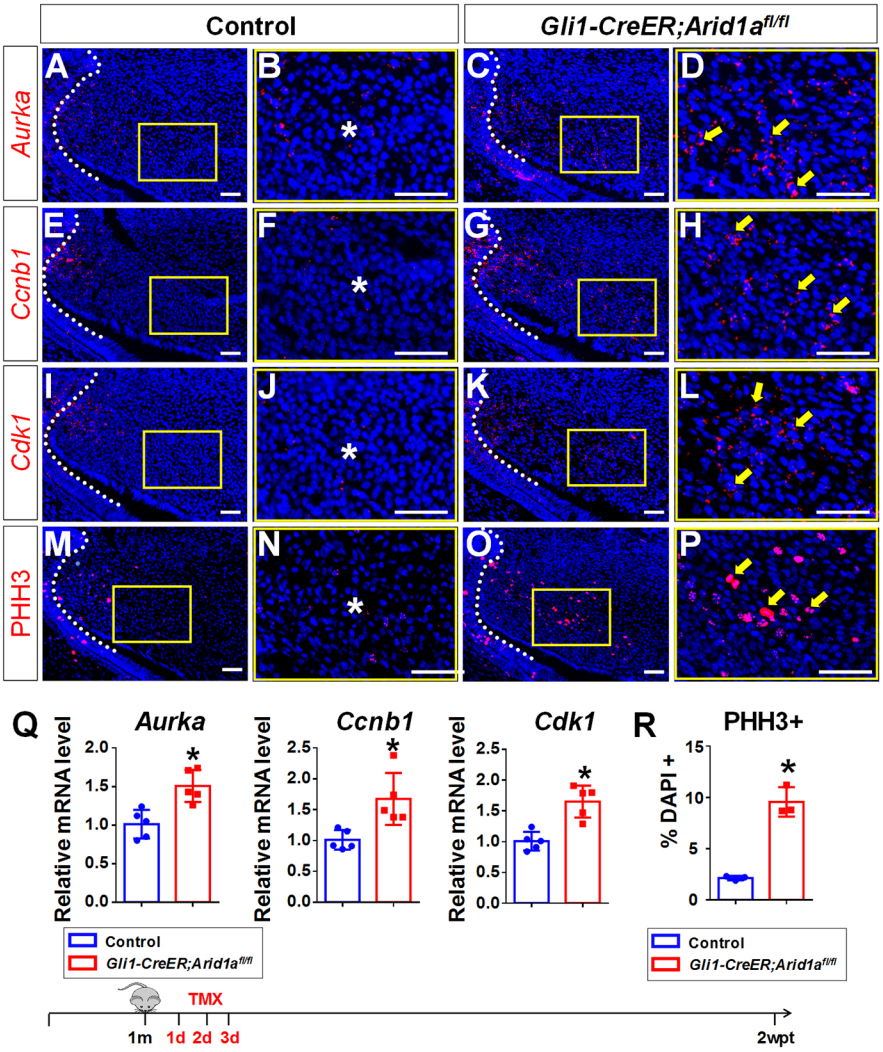

Fig. 5. Loss of *Arid1a* leads to upregulated Aurka-Cdk1 axis in the TAC region. (A-L) RNAscope *in situ* hybridization (red) of *Aurka* (A-D), *Ccnb1* (E-H) and *Cdk1* (I-L) of incisors from control and *Gli1-CreER;Arid1a*$^{fl/fl}$ mice 2 weeks after induction. B,D,F,H,J,L represent high-magnification images of boxes in A,C, E,G,I,K, respectively. (M-P) PHH3 immunostaining of incisors from control (M,N) and *Gli1-CreER;Arid1a*$^{fl/fl}$ mice (O,P) 2 weeks after induction. N, P represent high-magnification images of boxes in M, O, respectively. White dotted line outlines cervical loop. Yellow arrows indicate positive signal. Asterisk indicates no signal. *n*=3. (Q) qPCR of *Aurka*, *Ccnb1* and *Cdk1* in the incisor mesenchymal TAC region from control and *Gli1-CreER;Arid1a*$^{fl/fl}$ mice 2 weeks after induction. (R) Quantification of the percentage of pHH3+ cells in dental mesenchyme of incisors from control and *Gli1-CreER;Arid1a*$^{fl/fl}$ mice 2 weeks after induction. Data are mean±s.d., *n*=3, unpaired, two-tailed Student's *t*-test, **P*<0.05. Schematic at the bottom indicates induction protocol. wpt, week post-tamoxifen injection. Scale bars: 50 µm.

Ccnb1 and *Cdk1* using a chromatin immunoprecipitation (ChIP) assay with chromatin isolated from the proximal region of the incisor mesenchyme from control adult mice. Referring to published ChIP-seq data on Arid1a (Gatchalian et al., 2018; Sun et al., 2016a), we designed q-PCR primers targeting putative binding sites in the proximal promoter regions of *Aurka*, *Ccnb1* and *Cdk1* (Fig. 7B; Fig. S9). The promoter control element from a silent (*Ins1*) gene was used as a negative genomic control (Chandler et al., 2013). We found that Arid1a was enriched at the promoters of *Aurka*, *Ccnb1* and *Cdk1* in the proximal region of the adult mouse incisor mesenchyme (Fig. 7B). Furthermore, E2F4 is a transcriptional repressor that binds to promoters of cell cycle genes, and Arid1a has been reported to interact with E2F4 in murine MC3T3-E1 cells and mouse liver (Nagl et al., 2007; Sun et al., 2016a). Referring to published ChIP-seq data on E2F4 (MacIsaac et al., 2010) and Arid1a (Gatchalian et al., 2018; Sun et al., 2016a), we found that E2F4 and Arid1a share similar patterns of promoter occupancy at *Aurka*, *Ccnb1* and *Cdk1*. We further confirmed the interaction of Arid1a and E2F4 in the proximal incisor mesenchyme using co-immunoprecipitation (Fig. S10), which suggested that E2F4 may participate in the transcriptional repression of Arid1a at *Aurka*, *Ccnb1* and *Cdk1* as a potential co-repressor.

In summary, these data suggest that Arid1a represses the Aurka-Ccnb1-Cdk1 axis during the cell cycle exit of TACs. Loss of *Arid1a* overactivates the axis, leading to an expanded TAC population with compromised differentiation. The odontoblast differentiation and migration defects cause disorganized dentin formation at the proximal region of mouse incisor mesenchyme. Furthermore, the defective tissue homeostasis following the loss of *Arid1a* results in a reduced population of MSCs in adult mouse incisor (Fig. 7C).

DISCUSSION

A key feature of stem cell homeostasis is that the progeny of stem cells can initiate well-coordinated terminal differentiation after limited TAC divisions (Rangel-Huerta and Maldonado, 2017). Precise cell cycle regulation is crucial during the fate commitment of highly mitotic TACs. Mitotic kinases exert pivotal functions throughout mitotic progression (Schmit and Ahmad, 2007). Cdk1, the most prominent mitotic kinase, is a maturation-promoting factor, together with its cyclin binding partner Ccnb1. Once the complex forms and is activated, it phosphorylates multiple targets and promotes mitotic progression. Aurka belongs to an evolutionarily conserved family of serine/threonine kinases and is required for the separation of centrosomes and formation of the mitotic spindle (Schmit and Ahmad, 2007). Previous studies have shown that Aurka, Cdk1 and other mitotic kinases are part of a feedback activation loop during mitosis entry (Cazales et al., 2005; Van Horn et al., 2010). The activity of the Aurka-Ccnb1-Cdk1 axis peaks at mitosis and reduces during and after mitotic exit (Abdelbaki et al., 2020; Afonso et al., 2019; Lindon and Pines, 2004). As for the regulatory mechanisms that operate during mitotic progression,

Development (2021) 148, dev198838. doi:10.1242/dev.198838

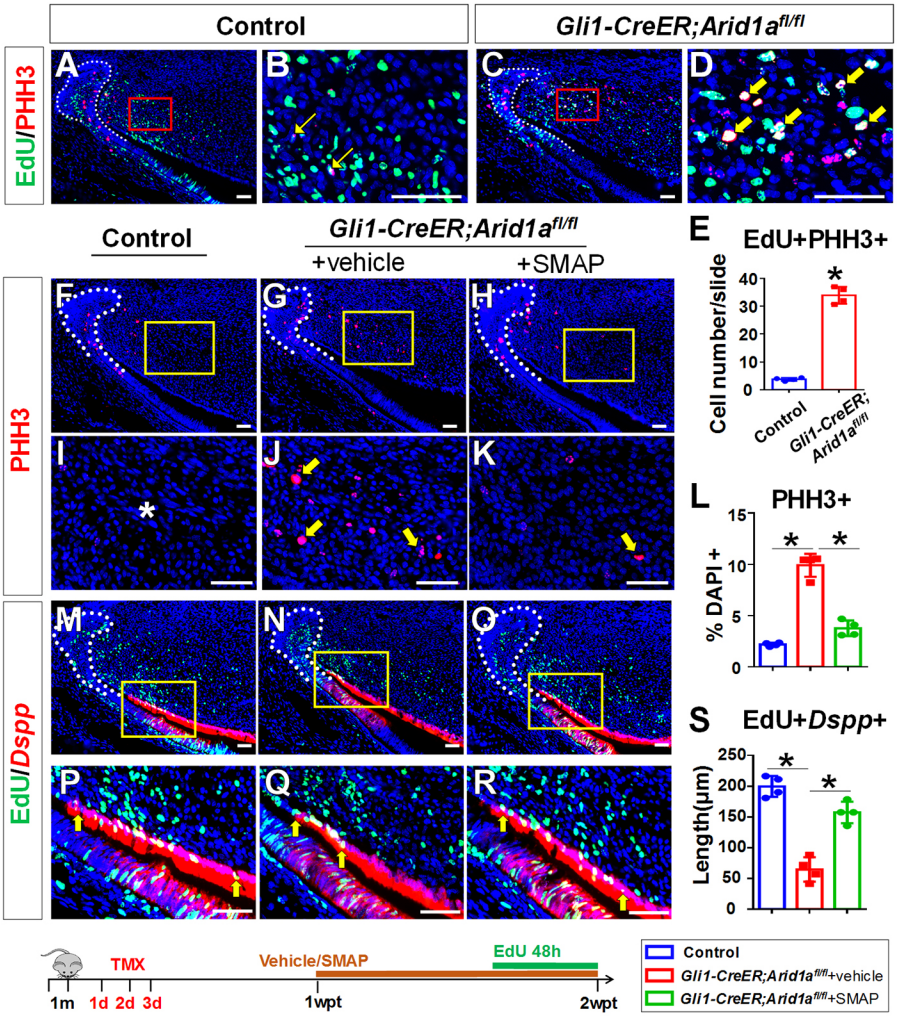

Fig. 6. Arid1a promotes the mitotic exit of TACs in mouse incisor. (A-D) Immunostaining of pHH3 (red) and EdU staining (green) of incisors from control (A,B) and *Gli1-CreER;Arid1a*$^{fl/fl}$ mice (C,D) 2 weeks after induction. B, D represent high-magnification images of boxes in A, B, respectively. White dotted line outlines cervical loop. Yellow arrows indicate EdU+PHH3+ cells. *n*=4. (E) Quantification of EdU+PHH3+ cells from control and *Gli1-CreER;Arid1a*$^{fl/fl}$ mouse incisors 2 weeks after induction. Data are mean±s.d., *n*=4, unpaired two-tailed Student's *t*-test, **P*<0.05. (F-K) PHH3 immunostaining of incisors from control (F,I) and *Gli1-CreER;Arid1a*$^{fl/fl}$ mice treated with vehicle (G,J) or SMAP (H,K) 2 weeks after induction. I,J,K represent high-magnification images of boxes in F, G,H, respectively. White dotted line outlines cervical loop. Yellow arrows indicate positive signal. Asterisk indicates no signal. *n*=4. (L) Quantification of the percentage of pHH3+ cells in dental mesenchyme of incisors from control and *Gli1-CreER;Arid1a*$^{fl/fl}$ mice treated with vehicle or SMAP 2 weeks after induction. Data are mean±s.d., *n*=4, one-way ANOVA, **P*<0.05. (M-R) RNAscope of *Dspp* (red) and EdU staining (green) of incisors from control (M, P) and *Gli1-CreER;Arid1a*$^{fl/fl}$ mice treated with vehicle (N,Q) or SMAP (O,R) 2 weeks after induction. P,Q,R represent high-magnification images of boxes in M,N,O, respectively. White dotted line outlines the cervical loop. Yellow arrows indicate positive signal. *n*=4. (S) Quantification of the overlapping length of EdU-labeled *Dspp*+ cells (distance between yellow arrows) from control and *Gli1-CreER;Arid1a*$^{fl/fl}$ mouse incisors treated with vehicle or SMAP 2 weeks after induction. Data are mean±s.d., *n*=4, one-way ANOVA, **P*<0.05. Schematic at the bottom indicates induction, EdU incorporation and vehicle/SMAP treatment protocol. wpt, week post-tamoxifen injection. Scale bars: 50 µm.

previous studies have focused on post-translational modifications, including phosphorylation, ubiquitylation and sumoylation (Cuijpers and Vertegaal, 2018). In the present work, we found that Arid1a binds to the promoters of *Aurka*, *Ccnb1* and *Cdk1* and might repress their gene transcription during the mitotic exit of TACs.

It is known that Arid1a modulates transcription via interacting with transcription factors, co-activators and co-repressors, which recognize DNA sequence-specific motifs (Dallas et al., 2000; Helming et al., 2014). Findings in the present study suggest that E2F4 might work with Arid1a as a potential co-factor at promoters of *Aurka*, *Ccnb1* and *Cdk1* during the cell cycle exit of TACs in the incisor mesenchyme. There remains work to be done in this area in the future, including detailed and comprehensive analysis of chromatin accessibility changes after loss of *Arid1a* in the mouse incisor and identification of co-factors working with Arid1a to control cell cycle progression. Several recent studies reported the emerging role of ARID1A in regulating enhancer-mediated gene expression in human colorectal cancer (Mathur et al., 2017) and neuroblastoma cells (Shi et al., 2020) and in preventing super-enhancer hyperactivation in endometrial epithelia (Wilson et al., 2020). These findings highlight the importance of Arid1a in homeostasis of multiple tissues as well as the context-dependent character of its function. Interestingly, loss of *Arid1a* leads to significant upregulation of *Aurka*, *Ccnb1* and *Cdk1* in the proximal region of the incisor mesenchyme, but not in the dental epithelium, consistent with the dominant regulatory role of Arid1a in mesenchyme to maintain incisor tissue homeostasis. There may be mechanisms in the epithelium that are able to compensate for the loss of *Arid1a*.

Due to a loss of *Arid1a*, TACs fail to exit the cell cycle and differentiate into odontoblasts normally to maintain incisor tissue homeostasis. This is consistent with a recent study demonstrating that loss of *Arid1a* enhances the proliferation and survival of liver cells after injury while somewhat attenuating tissue maturation (Sun et al., 2016b). The function of Arid1a in promoting the cell cycle exit and differentiation of TACs in the mouse incisor may be related to its tumor repressor role in many malignancies including endometrioid and clear-cell ovarian, gastric, colorectal and breast cancers (Kadoch et al., 2013). During cancer growth, the process of cancer stem cells giving rise to TACs is similar to that of normal tissue renewal, but cancer TACs then accumulate instead of differentiating, resulting in tumor growth (Sell, 2010). In the present study, using the mouse incisor as a model, we found that loss of *Arid1a* leads to upregulation of the Aurka-Ccnb1-Cdk1 axis, which might provide potential treatment targets for *ARID1A* mutation-associated cancer in the future.

Our findings concerning the mechanisms through which Arid1a limits the proliferation of TACs move beyond recent studies that have described epigenetic regulators and signaling pathways that promote the proliferation of TACs in the mouse incisor. For example, PRC1, which is a well-known epigenetic regulator, is

Development (2021) 148, dev198838. doi:10.1242/dev.198838

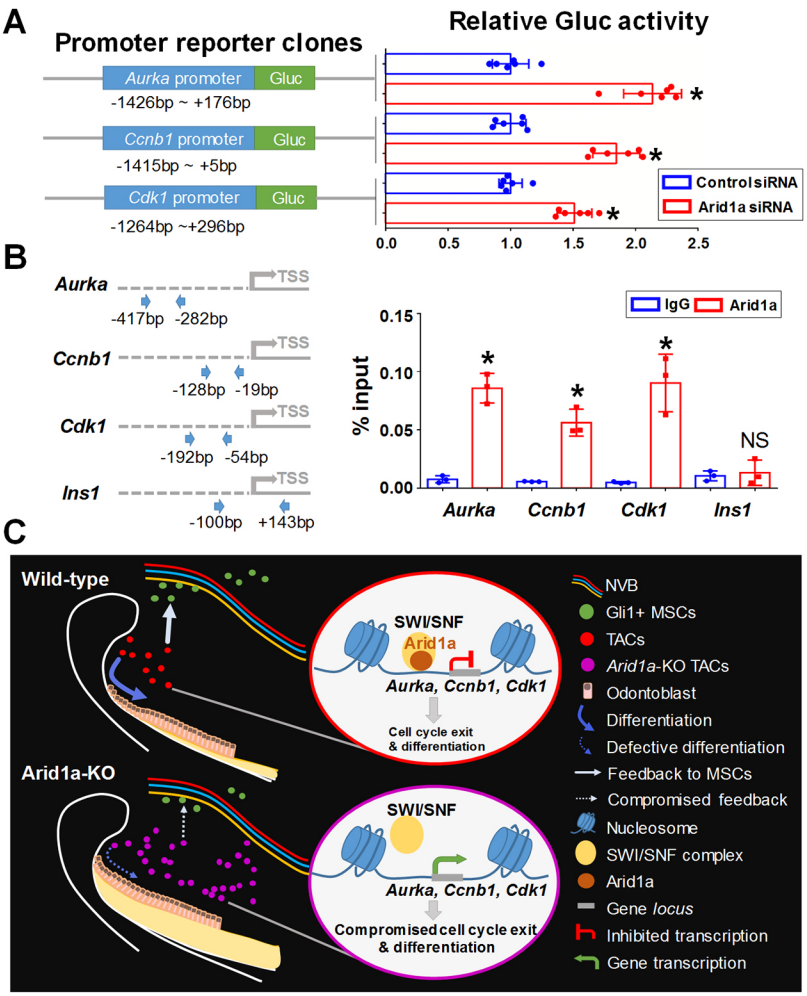

Fig. 7. Arid1a negatively regulates promoter activities of *Aurka*, *Ccnb1* and *Cdk1*. (A) The promoter reporter clones for mouse *Aurka*, *Ccnb1* and *Cdk1* in mammalian pEZX-PG04 vector with *Gaussia* luciferase reporter and SEAP tracking gene were transfected into ST2 mesenchymal stromal cell line. Then the cells were transfected with control siRNA or Arid1a siRNA. The cell culture medium was collected for secrete-pair dual luminescence assay. Using SEAP signal as an internal standard control, the normalized GLuc activity (GLuc/SEAP ratio) of all samples was compared. Each sample was used in duplicate reactions. Each group has six replicate samples. Data are mean±s.d., unpaired two-tailed Student's *t*-test, **P*<0.05. The experiment was performed in triplicate independently. (B) ChIP assay with chromatin isolated from the proximal region of the incisor mesenchyme from control adult mice using Arid1a antibody or IgG, followed by q-PCR with primers for amplifying a region at the promoter at *Aurka*, *Ccnb1* and *Cdk1* with promoter control element from a silent (*Ins1*) gene used as negative genomic control. Schematic on the left illustrates the location of the primers used to amplify the region at the promoters of *Aurka*, *Ccnb1*, *Cdk1* and *Ins1*. Data are mean ±s.d., *n*=3, unpaired, two-tailed Student's *t*-test, **P*<0.05. (C) Arid1a binds the promoter regions of *Aurka*, *Ccnb1* and *Cdk1* and represses their gene transcription during the cell cycle exit of TACs. Loss of *Arid1a* overactivates the Aurka-Cdk1 axis, leading to expanded TACs with compromised differentiation. The odontoblast differentiation and migration defects cause stacked dentin formation at the proximal region of mouse incisor mesenchyme. The defective homeostasis after loss of *Arid1a* ultimately leads to reduction of the MSC population.

highly expressed in mesenchymal TACs in mouse incisor; it maintains TAC proliferation by controlling Wnt/β-catenin signaling and inhibiting Cdkn2a while activating cyclin E2 and other positive cell-cycle regulators (An et al., 2018). Our recent study has shown that IGF signaling is important for Runx2+ niche cells, which reside between MSCs and TACs in the mouse incisor, to promote the proliferation of TACs (Chen et al., 2020). In addition, Notch signaling and Dlk1 are indispensable for maintaining TACs in the mouse incisor (Walker et al., 2019). These studies have highlighted the positive regulatory mechanisms by these factors in promoting TAC proliferation in the mouse incisor. Interestingly, the present study has discovered that Arid1a is highly expressed in TACs in the adult mouse incisor and may work as a negative cell cycle regulator to repress the Aurka-Ccnb1-Cdk1 axis. Loss of *Arid1a* overactivates the Aurka-Cdk1 axis, leading to increased mitotic TACs at the proximal end of the mouse incisor. This is a different and previously unknown epigenetic mechanism that regulates TAC proliferation in the mouse incisor. These findings together contribute to a comprehensive understanding of the regulatory network of TACs and specifically improve our understanding of the negative regulatory mechanism that controls the proliferation of TACs during tissue homeostasis.

Interestingly, although Arid1a is not expressed in the incisor MSC population, defective tissue homeostasis following the loss of *Arid1a* results in a reduction of MSCs. This reduction may be caused by the overactivated proliferation of TACs after loss of *Arid1a* through negative feedback, which is distinct from previous studies on the positive feedback mechanism between TACs and MSCs. For example, loss of TAC proliferation caused by deletion of *Ring1b* (also known as *Rnf2*) leads to reduction of MSCs via a positive feedback mechanism (An et al., 2018); reduced TAC proliferation after loss of *Runx2* in the Gli1+ lineage also decreases the MSC population via positive feedback (Chen et al., 2020). The potential negative feedback between increased TACs and reduced MSCs found in our study highlights the complex nature of TAC-MSC crosstalk, which may involve both positive and negative feedback mechanisms. However, the reduction of MSCs could also be due to systemic effects of the reduced odontoblast differentiation and incisor growth, which could signal to the MSCs to generate more TACs than usual and deplete the MSCs in the process. Therefore, the precise mechanism underlying the reduction in MSCs after loss of *Arid1a* should be explored further in the future. The finding that Arid1a helps to maintain the stem cell pool size in our study is also consistent with its role in the hematopoietic system: the proportion of non-cycling, quiescent hematopoietic stem cells is significantly reduced in *Arid1a*-deficient bone marrow (Han et al., 2019). These data demonstrate that Arid1a is critical for stem cell-supported tissue homeostasis.

In conclusion, our study has unveiled the function of Arid1a in the growth and homeostasis of the adult mouse incisor. We show that Arid1a promotes cell cycle exit and differentiation of TACs during tissue homeostasis. Furthermore, we have discovered that Arid1a binds to the promoters of *Aurka*, *Ccnb1* and *Cdk1* and may participate in their transcriptional repression during the mitotic exit

Development (2021) 148, dev198838. doi:10.1242/dev.198838

of TACs. Loss of *Arid1a* overactivates the Aurka-Cdk1 axis, leading to an expanded population of mitotic TACs but compromising their differentiation ability. The defective tissue homeostasis following the loss of *Arid1a* ultimately leads to a reduction of the MSC population. Our study thus provides new mechanistic insights into how Arid1a serves as a negative cell cycle regulator to coordinate TAC-MSC interaction and maintain the homeostasis of MSCs, TACs and their differentiated progeny in adult mouse incisor.

MATERIALS AND METHODS

Generation of transgenic mouse lines

Arid1a$^{fl/fl}$ (Gao et al., 2008), *Gli1-CreER* (Ahn and Joyner, 2004), *tdTomato* (Madisen et al., 2010), *Sox2-CreER* (Li et al., 2015) and *Gli1-lacZ* (Bai et al., 2002) mouse lines were used and cross-bred in this study. All mouse lines used are listed in Table S1. All mice were housed in pathogen-free conditions and euthanized by carbon dioxide overdose followed by cervical dislocation. All animal studies were approved by the Institutional Animal Care and Use Committee at the University of Southern California. Both male and female mice were included in our experiments.

Tamoxifen and SMAP administration

Tamoxifen (Sigma-Aldrich, T5648) was dissolved in corn oil (Sigma-Aldrich, C8267) at 20 mg/ml. At 1 month of age, control and *Gli1-CreER;Arid1a*$^{fl/fl}$ or *Sox2-CreER;Arid1a*$^{fl/fl}$ mice were injected intraperitoneally at a dosage of 1.5 mg/10 g body weight. DT-061 (SMAP, S8774) was purchased from Selleck. It was administered to *Gli1-CreER;Arid1a*$^{fl/fl}$ mice at a dosage of 5 mg/kg via oral gavage 1 week after tamoxifen injection.

Histological analysis, immunofluorescence and *in situ* hybridization

Mouse mandibles were dissected and fixed in 4% paraformaldehyde (PFA) overnight, followed by decalcification in 10% EDTA in PBS for 3-6 weeks depending on the age of the samples. For Hematoxylin and Eosin (H&E) staining, the decalcified mandibles were dehydrated in an ethanol and xylene series and embedded in paraffin, with sections cut at a thickness of 4 µm using a microtome (Leica, RM2235 ccwUS). For immunofluorescence (IF) and *in situ* hybridization (ISH) analysis, the decalcified mandibles were dehydrated in serial sucrose/PBS solutions and embedded in OCT compound (Tissue-Tek, Sakura). OCT-embedded samples were cryosectioned at 8 µm using a cryostat (Leica CM1850) followed by staining. For IF staining, cryosections were soaked in blocking solution (PerkinElmer, FP1012) for 1 h at room temperature and then incubated with primary antibodies diluted in blocking solution at 4°C overnight. After washing three times in PBS, the sections were incubated with Alexa-conjugated secondary antibody (Invitrogen) and counterstained with DAPI. For ISH analysis, cryosections were stained with RNAscope Multiplex Fluorescent kit (Advanced Cell Diagnostics, 320850) according to the manufacturer's instructions. All of the antibodies and probes used in the present study are listed in Table S1.

EdU incorporation, staining and TUNEL assays

Gli1-CreER;Arid1a$^{fl/fl}$ mice and littermate controls were injected with EdU (25 µg/g body weight) intraperitoneally 2 or 48 h before being euthanized. The mandibles were fixed and decalcified. Click-iT™ plus EdU cell proliferation kit (Thermo Fisher Scientific, C10637) was used on the cryosections for *in situ* EdU detection according to the manufacturer's instructions. Cell apoptosis was detected using a TUNEL assay (Click-iT™ Plus TUNEL Assay for In Situ Apoptosis Detection, Thermo Fisher Scientific, C10617) according to the manufacturer's protocol.

RNA-sequencing analysis and qPCR

Two weeks after tamoxifen induction, first mandibular molars from *Gli1-CreER;Arid1a*$^{fl/fl}$ mice and littermate controls were dissected out. The proximal end of incisor mesenchyme was then collected and RNA was extracted using an RNeasy Micro Kit (Qiagen, 74004). For RNA-sequencing analysis, cDNA library preparation and sequencing were performed at the Technology Center for Genomics & Bioinformatics at the University of California, Los Angeles (UCLA), USA. Raw reads were trimmed and aligned with the mm10 genome. Differential analysis was performed by selecting transcripts with $P \leq 0.01$, fold change <-1.5 or <1.5.

For qPCR analysis, RNA was reverse-transcribed with an iScript™ cDNA Synthesis Kit (Bio-Rad, 1708891) and the relative amounts of each mRNA transcript were analyzed using the CFX96 Real-Time System (Bio-Rad, iCycler) with SsoAdvanced™ Universal SYBR® Green Supermix (Bio-Rad, 1725270). The relative expression levels of particular genes were compared across groups using the $2^{-\Delta\Delta Ct}$ method, with the expression of β-actin as an internal control. Primer sequences were obtained from PrimerBank (http://pga.mgh.harvard.edu/primerbank/) and are listed in Table S1.

Dual luminescence assay

Stromal cell line ST2 (Amzaleg et al., 2018) was cultured in RPMI 1640 medium (Thermo Fisher Scientific, 11875093) with 10% fetal bovine serum (Thermo Fisher Scientific, 12662029) at 37°C in a 5% CO_2 incubator. Cells were plated onto 6-well plates 24 h before transfection. The promoter reporter clones for mouse Aurka (Genecopoeia, MPRM38008-PG04-50), Ccnb1 (Genecopoeia, MPRM49947-PG04-50) and Cdk1 (Genecopoeia, MPRM39244-PG04-50) in mammalian pEZX-PG04 vector with *Gaussia* luciferase reporter and SEAP tracking gene were transfected using EndoFectin™ Max transfection reagent (Genecopoeia, EF013) according to the manufacturer's protocol. After another 24 h incubation, the cells were plated onto 24-well plates for siRNA transfection. Arid1a siRNA (Qiagen, 1027418, pooled #1 Mm_Arid1a_5 FlexiTube siRNA SI02676058 and #2 Mm_Arid1a_6 FlexiTube siRNA SI02696771), control siRNA (Thermo Fisher Scientific, 4390844), lipofectamine™ RNAiMAX (Thermo Fisher Scientific, 13778075) and Opti-MEM™ I Reduced Serum Medium (Thermo Fisher Scientific, 31985062) were used in this study. The final concentration of control or Arid1a siRNA was 25 µM during reverse transfection. After 12 h incubation, the transfected cells were changed into fresh medium. After another 24 h incubation, the cell culture medium was gently collected for Secrete-Pair Dual Luminescence Assay (Genecopoeia, LF033) according to the manufacturer's instructions. Each group had six replicate samples. Each sample was used in duplicate reactions. Using SEAP signal as an internal standard control, the normalized GLuc activity (GLuc/SEAP ratio) of all samples was compared. Independent experiments were repeated in triplicate.

ChIP assay

The proximal incisor mesenchyme was collected from wild-type mice and fixed with formaldehyde. SimpleChIP® Plus Enzymatic Chromatin IP Kit (Magnetic Beads; Cell Signaling Technology, #9005), anti-Arid1a antibody (Cell Signaling Technology, 12354, 1:100), and rabbit IgG (Cell Signaling Technology, 2729, same concentration as the test antibody) were used following the manufacturer's instructions. The enrichment of particular DNA sequences during immunoprecipitation was analyzed by qPCR. The ChIP primers amplified regions at the proximal promoters of *Aurka*, *Ccnb1* and *Cdk1* as listed in Table S1. The promoter control element from a silent (*Ins1*) gene was used as negative genomic control (Chandler et al., 2013).

Co-immunoprecipitation

The proximal incisor mesenchyme was collected from wild-type mice and lysed in lysis buffer [50 mM Tris-HCl (pH 7.5), 150 mM NaCl, 2 mM EDTA (pH 8.0), 1 mM PMSF, 1% NP-40, 5% glycerol]. After preclearing using protein A-Sepharose (VWR, CA97067-898), the lysates were subjected to immunoprecipitation with anti-Arid1a antibody (Cell Signaling Technology, 12354, 1:100) or Rabbit (DA1E) mAb IgG XP® Isotype Control (Cell Signaling Technology, 3900) and protein A-Sepharose (VWR, CA97067-898). Immune complexes were washed and subjected to immunoblotting with anti-Arid1a (Santa Cruz Biotechnology, sc-32761 HRP) or anti-E2F4 (Sigma-Aldrich, 05-312) antibodies. Western blot was performed per standard protocol and signals were detected using Azure 300 (Azure Biosystems).

Development (2021) 148, dev198838. doi:10.1242/dev.198838

Statistical analysis

All statistical analyses were performed with GraphPad Prism and are presented as individual data points and mean±s.d. unless otherwise stated. Unpaired two-tailed Student's *t*-test or one-way ANOVA with Brown-Forsythe test was applied for comparisons, with $P<0.05$ considered statistically significant. $N\geq3$ for all samples; all experiments were repeated in triplicate unless otherwise stated.

Acknowledgements

We acknowledge Dr Bridget Samuels and Ms Linda Hattemer for critical editing of the manuscript, University of Southern California (USC) Libraries Bioinformatics Service for assisting with data analysis, and the USC Office of Research and the USC Libraries for supporting our access to bioinformatics software and computing resources.

Competing interests

The authors declare no competing or financial interests.

Author contributions

Conceptualization: J.D., X.J., Y.C.; Methodology: J.D., J.J., S.C., Y.Y., J.F., T.-V.H., P.S., X.J., Y.C.; Validation: J.D., J.J., S.C., Y.Y., J.F., Y.C.; Formal analysis: J.D., J.J., S.C., Y.Y., Y.C.; Investigation: J.D., S.C., Y.Y., J.F., T.-V.H., X.J., Y.C.; Resources: Y.C.; Data curation: J.D., J.J., S.C., Y.Y., T.-V.H., P.S., J.X., Y.C.; Writing - original draft: J.D., Y.C.; Writing - review & editing: J.D., J.J., S.C., Y.Y., J.F., X.J., Y.C.; Visualization: J.D., Y.Y., J.F., Y.C.; Supervision: J.X., Y.C.; Project administration: P.S., J.X., Y.C.; Funding acquisition: Y.C.

Funding

This study was supported by funding from the National Institute of Dental and Craniofacial Research, National Institutes of Health (R01 DE025221, R01 DE022503, U01 DE028729 and R01 DE012711 to Y.C.). Deposited in PMC for release after 12 months.

Data availability

RNA-sequencing data have been deposited in GEO under accession number GSE166800.

Peer review history

The peer review history is available online at https://journals.biologists.com/dev/article-lookup/doi/10.1242/dev.198838

References

Abdelbaki, A., Akman, H. B., Poteau, M., Grant, R., Gavet, O., Guarguaglini, G. and Lindon, C. (2020). AURKA destruction is decoupled from its activity at mitotic exit but is essential to suppress interphase activity. *J. Cell Sci.* **133**, jcs243071. doi:10.1242/jcs.243071

Afonso, O., Castellani, C. M., Cheeseman, L. P., Ferreira, J. G., Orr, B., Ferreira, L. T., Chambers, J. J., Morais-de-Sa, E., Maresca, T. J. and Maiato, H. (2019). Spatiotemporal control of mitotic exit during anaphase by an aurora B-Cdk1 crosstalk. *Elife* **8**, e47646. doi:10.7554/eLife.47646.052

Ahn, S. and Joyner, A. L. (2004). Dynamic changes in the response of cells to positive hedgehog signaling during mouse limb patterning. *Cell* **118**, 505-516. doi:10.1016/j.cell.2004.07.023

Amzaleg, Y., Ji, J., Kittivanichkul, D., E Törnqvist, A., Windahl, S., Sabag, E., Khalid, A. B., Sternberg, H., West, M., Katzenellenbogen, J. A. et al. (2018). Estrogens and selective estrogen receptor modulators differentially antagonize Runx2 in ST2 mesenchymal progenitor cells. *J. Steroid Biochem. Mol. Biol.* **183**, 10-17. doi:10.1016/j.jsbmb.2018.05.002

An, Z., Akily, B., Sabalic, M., Zong, G., Chai, Y. and Sharpe, P. T. (2018). Regulation of mesenchymal stem to transit-amplifying cell transition in the continuously growing mouse incisor. *Cell Rep.* **23**, 3102-3111. doi:10.1016/j.celrep.2018.05.001

Arnold, K., Sarkar, A., Yram, M. A., Polo, J. M., Bronson, R., Sengupta, S., Seandel, M., Geijsen, N. and Hochedlinger, K. (2011). Sox2(+) adult stem and progenitor cells are important for tissue regeneration and survival of mice. *Cell Stem Cell* **9**, 317-329. doi:10.1016/j.stem.2011.09.001

Bai, C. B., Auerbach, W., Lee, J. S., Stephen, D. and Joyner, A. L. (2002). Gli2, but not Gli1, is required for initial Shh signaling and ectopic activation of the Shh pathway. *Development* **129**, 4753-4761.

Blank, U., Karlsson, G. and Karlsson, S. (2008). Signaling pathways governing stem-cell fate. *Blood* **111**, 492-503. doi:10.1182/blood-2007-07-075168

Busch, K., Klapproth, K., Barile, M., Flossdorf, M., Holland-Letz, T., Schlenner, S. M., Reth, M., Hofer, T. and Rodewald, H. R. (2015). Fundamental properties of unperturbed haematopoiesis from stem cells in vivo. *Nature* **518**, 542-546. doi:10.1038/nature14242

Cakouros, D. and Gronthos, S. (2020). Epigenetic regulators of mesenchymal stem/stromal cell lineage determination. *Curr. Osteoporos Rep.* **18**, 597-605. doi:10.1007/s11914-020-00616-0

Cazales, M., Schmitt, E., Montembault, E., Dozier, C., Prigent, C. and Ducommun, B. (2005). CDC25B phosphorylation by Aurora-A occurs at the G2/M transition and is inhibited by DNA damage. *Cell Cycle* **4**, 1233-1238. doi:10.4161/cc.4.9.1964

Chacon-Martinez, C. A., Koester, J. and Wickstrom, S. A. (2018). Signaling in the stem cell niche: regulating cell fate, function and plasticity. *Development* **145**, dev165399. doi:10.1242/dev.165399

Chandler, R. L. and Magnuson, T. (2016). The SWI/SNF BAF-A complex is essential for neural crest development. *Dev. Biol.* **411**, 15-24. doi:10.1016/j.ydbio.2016.01.015

Chandler, R. L., Brennan, J., Schisler, J. C., Serber, D., Patterson, C. and Magnuson, T. (2013). ARID1a-DNA interactions are required for promoter occupancy by SWI/SNF. *Mol. Cell. Biol.* **33**, 265-280. doi:10.1128/MCB.01008-12

Chen, S., Jing, J., Yuan, Y., Feng, J., Han, X., Wen, Q., Ho, T.-V., Lee, C. and Chai, Y. (2020). Runx2+ Niche cells maintain incisor mesenchymal tissue homeostasis through IGF signaling. *Cell Rep* **32**, 108007. doi:10.1016/j.celrep.2020.108007

Childs, R., Chernoff, A., Contentin, N., Bahceci, E., Schrump, D., Leitman, S., Read, E. J., Tisdale, J., Dunbar, C., Linehan, W. M. et al. (2000). Regression of metastatic renal-cell carcinoma after nonmyeloablative allogeneic peripheral-blood stem-cell transplantation. *N. Engl. J. Med.* **343**, 750-758. doi:10.1056/NEJM200009143431101

Cuijpers, S. A. G. and Vertegaal, A. C. O. (2018). Guiding mitotic progression by crosstalk between post-translational modifications. *Trends Biochem. Sci.* **43**, 251-268. doi:10.1016/j.tibs.2018.02.004

Dallas, P. B., Pacchione, S., Wilsker, D., Bowrin, V., Kobayashi, R. and Moran, E. (2000). The human SWI-SNF complex protein p270 is an ARID family member with non-sequence-specific DNA binding activity. *Mol. Cell. Biol.* **20**, 3137-3146. doi:10.1128/MCB.20.9.3137-3146.2000

Feng, J., Mantesso, A., De Bari, C., Nishiyama, A. and Sharpe, P. T. (2011). Dual origin of mesenchymal stem cells contributing to organ growth and repair. *Proc. Natl. Acad. Sci. USA* **108**, 6503-6508. doi:10.1073/pnas.1015449108

Feng, J., Jing, J., Li, J., Zhao, H., Punj, V., Zhang, T., Xu, J. and Chai, Y. (2017). BMP signaling orchestrates a transcriptional network to control the fate of mesenchymal stem cells in mice. *Development* **144**, 2560-2569. doi:10.1242/dev.150136

Gao, X., Tate, P., Hu, P., Tjian, R., Skarnes, W. C. and Wang, Z. (2008). ES cell pluripotency and germ-layer formation require the SWI/SNF chromatin remodeling component BAF250a. *Proc. Natl. Acad. Sci. USA* **105**, 6656-6661. doi:10.1073/pnas.0801802105

Gatchalian, J., Malik, S., Ho, J., Lee, D. S., Kelso, T. W. R., Shokhirev, M. N., Dixon, J. R. and Hargreaves, D. C. (2018). A non-canonical BRD9-containing BAF chromatin remodeling complex regulates naive pluripotency in mouse embryonic stem cells. *Nat. Commun.* **9**, 5139. doi:10.1038/s41467-018-07528-9

Han, L., Madan, V., Mayakonda, A., Dakle, P., Woon, T. W., Shyamsunder, P., Nordin, H. B. M., Cao, Z., Sundaresan, J., Lei, I. et al. (2019). Chromatin remodeling mediated by ARID1A is indispensable for normal hematopoiesis in mice. *Leukemia* **33**, 2291-2305. doi:10.1038/s41375-019-0438-4

Helming, K. C., Wang, X. and Roberts, C. W. M. (2014). Vulnerabilities of mutant SWI/SNF complexes in cancer. *Cancer Cell* **26**, 309-317. doi:10.1016/j.ccr.2014.07.018

Hiramatsu, Y., Fukuda, A., Ogawa, S., Goto, N., Ikuta, K., Tsuda, M., Matsumoto, Y., Kimura, Y., Yoshioka, T., Takada, Y. et al. (2019). Arid1a is essential for intestinal stem cells through Sox9 regulation. *Proc. Natl. Acad. Sci. USA* **116**, 1704-1713. doi:10.1073/pnas.1804858116

Hota, S. K. and Bruneau, B. G. (2016). ATP-dependent chromatin remodeling during mammalian development. *Development* **143**, 2882-2897. doi:10.1242/dev.128892

Hsu, Y. C., Li, L. and Fuchs, E. (2014). Transit-amplifying cells orchestrate stem cell activity and tissue regeneration. *Cell* **157**, 935-949. doi:10.1016/j.cell.2014.02.057

Jing, J., Feng, J., Li, J., Zhao, H., Ho, T. V., He, J., Yuan, Y., Guo, T., Du, J., Urata, M. et al. (2021). Reciprocal interaction between mesenchymal stem cells and transit amplifying cells regulates tissue homeostasis. *Elife* **10**, e59459. doi:10.7554/eLife.59459

Juuri, E., Saito, K., Ahtiainen, L., Seidel, K., Tummers, M., Hochedlinger, K., Klein, O. D., Thesleff, I. and Michon, F. (2012). Sox2+ stem cells contribute to all epithelial lineages of the tooth via Sfrp5+ progenitors. *Dev. Cell* **23**, 317-328. doi:10.1016/j.devcel.2012.05.012

Juuri, E., Jussila, M., Seidel, K., Holmes, S., Wu, P., Richman, J., Heikinheimo, K., Chuong, C. M., Arnold, K., Hochedlinger, K. et al. (2013). Sox2 marks epithelial competence to generate teeth in mammals and reptiles. *Development* **140**, 1424-1432. doi:10.1242/dev.089599

Kadoch, C., Hargreaves, D. C., Hodges, C., Elias, L., Ho, L., Ranish, J. and Crabtree, G. R. (2013). Proteomic and bioinformatic analysis of mammalian SWI/SNF complexes identifies extensive roles in human malignancy. *Nat. Genet.* **45**, 592-601. doi:10.1038/ng.2628

Kaukua, N., Shahidi, M. K., Konstantinidou, C., Dyachuk, V., Kaucka, M., Furlan, A., An, Z., Wang, L., Hultman, I., Ahrlund-Richter, L. et al. (2014). Glial origin of mesenchymal stem cells in a tooth model system. *Nature* **513**, 551-554. doi:10.1038/nature13536

Li, J., Feng, J., Liu, Y., Ho, T. V., Grimes, W., Ho, H. A., Park, S., Wang, S. and Chai, Y. (2015). BMP-SHH signaling network controls epithelial stem cell fate via regulation of its niche in the developing tooth. *Dev. Cell* **33**, 125-135. doi:10.1016/j.devcel.2015.02.021

Lindon, C. and Pines, J. (2004). Ordered proteolysis in anaphase inactivates Plk1 to contribute to proper mitotic exit in human cells. *J. Cell Biol.* **164**, 233-241. doi:10.1083/jcb.200309035

Liu, J., Liu, S., Gao, H., Han, L., Chu, X., Sheng, Y., Shou, W., Wang, Y., Liu, Y., Wan, J. et al. (2020). Genome-wide studies reveal the essential and opposite roles of ARID1A in controlling human cardiogenesis and neurogenesis from pluripotent stem cells. *Genome Biol.* **21**, 169. doi:10.1186/s13059-020-02082-4

MacIsaac, K. D., Lo, K. A., Gordon, W., Motola, S., Mazor, T. and Fraenkel, E. (2010). A quantitative model of transcriptional regulation reveals the influence of binding location on expression. *PLoS Comput. Biol.* **6**, e1000773. doi:10.1371/journal.pcbi.1000773

Madisen, L., Zwingman, T. A., Sunkin, S. M., Oh, S. W., Zariwala, H. A., Gu, H., Ng, L. L., Palmiter, R. D., Hawrylycz, M. J., Jones, A. R. et al. (2010). A robust and high-throughput Cre reporting and characterization system for the whole mouse brain. *Nat. Neurosci.* **13**, 133-140. doi:10.1038/nn.2467

Mathur, R., Alver, B. H., San Roman, A. K., Wilson, B. G., Wang, X. F., Agoston, A. T., Park, P. J., Shivdasani, R. A. and Roberts, C. W. M. (2017). ARID1A loss impairs enhancer-mediated gene regulation and drives colon cancer in mice. *Nat. Genet.* **49**, 296-302. doi:10.1038/ng.3744

Menon, D. U., Shibata, Y., Mu, W. and Magnuson, T. (2019). Mammalian SWI/SNF collaborates with a polycomb-associated protein to regulate male germline transcription in the mouse. *Development* **146**, dev174094. doi:10.1242/dev.174094

Morrison, S. J. and Spradling, A. C. (2008). Stem cells and niches: mechanisms that promote stem cell maintenance throughout life. *Cell* **132**, 598-611. doi:10.1016/j.cell.2008.01.038

Morrison, S. J., Shah, N. M. and Anderson, D. J. (1997). Regulatory mechanisms in stem cell biology. *Cell* **88**, 287-298. doi:10.1016/S0092-8674(00)81867-X

Nagl, N. G., Jr., Wang, X., Patsialou, A., Van Scoy, M. and Moran, E. (2007). Distinct mammalian SWI/SNF chromatin remodeling complexes with opposing roles in cell-cycle control. *EMBO J.* **26**, 752-763. doi:10.1038/sj.emboj.7601541

Rangel-Huerta, E. and Maldonado, E. (2017). Transit-amplifying cells in the fast lane from stem cells towards differentiation. *Stem Cells Int* **2017**, 7602951. doi:10.1155/2017/7602951

Ruijtenberg, S. and van den Heuvel, S. (2016). Coordinating cell proliferation and differentiation: Antagonism between cell cycle regulators and cell type-specific gene expression. *Cell Cycle* **15**, 196-212. doi:10.1080/15384101.2015.1120925

Schmit, T. L. and Ahmad, N. (2007). Regulation of mitosis via mitotic kinases: new opportunities for cancer management. *Mol. Cancer Ther.* **6**, 1920-1931. doi:10.1158/1535-7163.MCT-06-0781

Seidel, K., Ahn, C. P., Lyons, D., Nee, A., Ting, K., Brownell, I., Cao, T., Carano, R. A., Curran, T., Schober, M. et al. (2010). Hedgehog signaling regulates the generation of ameloblast progenitors in the continuously growing mouse incisor. *Development* **137**, 3753-3761. doi:10.1242/dev.056358

Sell, S. (2010). On the stem cell origin of cancer. *Am. J. Pathol.* **176**, 2584-2494. doi:10.2353/ajpath.2010.091064

Shi, C., Yuan, Y., Guo, Y., Jing, J., Ho, T. V., Han, X., Li, J., Feng, J. and Chai, Y. (2019). BMP Signaling in regulating mesenchymal stem cells in incisor homeostasis. *J. Dent. Res.* **98**, 904-911. doi:10.1177/0022034519850812

Shi, H., Tao, T., Abraham, B. J., Durbin, A. D., Zimmerman, M. W., Kadoch, C. and Look, A. T. (2020). ARID1A loss in neuroblastoma promotes the adrenergic-to-mesenchymal transition by regulating enhancer-mediated gene expression. *Sci. Adv.* **6**, eaaz3440. doi:10.1126/sciadv.aaz3440

Sun, J. L., Ramos, A., Chapman, B., Johnnidis, J. B., Le, L., Ho, Y. J., Klein, A., Hofmann, O. and Camargo, F. D. (2014). Clonal dynamics of native haematopoiesis. *Nature* **514**, 322. doi:10.1038/nature13824

Sun, X., Chuang, J.-C., Kanchwala, M., Wu, L., Celen, C., Li, L., Liang, H., Zhang, S., Maples, T., Nguyen, et al. (2016a). Suppression of the SWI/SNF component Arid1a promotes mammalian regeneration. *Cell Stem Cell* **18**, 456-466. doi:10.1016/j.stem.2016.03.001

Sun, X., Chuang, J. C., Kanchwala, M., Wu, L., Celen, C., Li, L., Liang, H., Zhang, S., Maples, T., Nguyen, L. H. et al. (2016b). Suppression of the SWI/SNF component arid1a promotes mammalian regeneration. *Cell Stem Cell* **18**, 456-466. doi:10.1016/j.stem.2016.03.001

Suryo Rahmanto, Y., Jung, J. G., Wu, R. C., Kobayashi, Y., Heaphy, C. M., Meeker, A. K., Wang, T. L. and Shih Ie, M. (2016). Inactivating ARID1A tumor suppressor enhances TERT transcription and maintains telomere length in cancer cells. *J. Biol. Chem.* **291**, 9690-9699. doi:10.1074/jbc.M115.707612

Thomas, E. D. (1975). Bone marrow transplantation: prospects for leukemia and other conditions. *Proc. Inst. Med. Chic.* **30**, 256-258.

Van Horn, R. D., Chu, S., Fan, L., Yin, T., Du, J., Beckmann, R., Mader, M., Zhu, G., Toth, J., Blanchard, K. et al. (2010). Cdk1 activity is required for mitotic activation of aurora A during G2/M transition of human cells. *J. Biol. Chem.* **285**, 21849-21857. doi:10.1074/jbc.M110.141010

Walker, J. V., Zhuang, H., Singer, D., Illsley, C. S., Kok, W. L., Sivaraj, K. K., Gao, Y., Bolton, C., Liu, Y., Zhao, M. et al. (2019). Transit amplifying cells coordinate mouse incisor mesenchymal stem cell activation. *Nat. Commun.* **10**, 3596. doi:10.1038/s41467-019-11611-0

Wilson, B. G. and Roberts, C. W. (2011). SWI/SNF nucleosome remodellers and cancer. *Nat. Rev. Cancer* **11**, 481-492. doi:10.1038/nrc3068

Wilson, M. R., Reske, J. J., Holladay, J., Wilber, G. E., Rhodes, M., Koeman, J., Adams, M., Johnson, B., Su, R. W., Joshi, N. R. et al. (2019). ARID1A and PI3-kinase pathway mutations in the endometrium drive epithelial transdifferentiation and collective invasion. *Nat. Commun.* **10**, 3554. doi:10.1038/s41467-019-11403-6

Wilson, M. R., Reske, J. J., Holladay, J., Neupane, S., Ngo, J., Cuthrell, N., Wegener, M., Rhodes, M., Adams, M., Sheridan, R. et al. (2020). ARID1A Mutations Promote P300-Dependent Endometrial Invasion through Super-Enhancer Hyperacetylation. *Cell Rep* **33**, 108366. doi:10.1016/j.celrep.2020.108366

Wlodarchak, N. and Xing, Y. (2016). PP2A as a master regulator of the cell cycle. *Crit. Rev. Biochem. Mol. Biol.* **51**, 162-184. doi:10.3109/10409238.2016.1143913

Wu, H. and Sun, Y. E. (2006). Epigenetic regulation of stem cell differentiation. *Pediatr. Res.* **59**, 21R-25R. doi:10.1203/01.pdr.0000203565.76028.2a

Zhang, B. and Hsu, Y. C. (2017). Emerging roles of transit-amplifying cells in tissue regeneration and cancer. *Wiley Interdiscip Rev. Dev. Biol.* **6**, e282. doi:10.1002/wdev.282

Zhao, H., Feng, J., Seidel, K., Shi, S., Klein, O., Sharpe, P. and Chai, Y. (2014). Secretion of shh by a neurovascular bundle niche supports mesenchymal stem cell homeostasis in the adult mouse incisor. *Cell Stem Cell* **14**, 160-173. doi:10.1016/j.stem.2013.12.013